

Short Communication

## Electrochemical Study of Inhibition Effect of a Schiff Base towards Magnesium Alloy Corrosion

Yuhang Guo<sup>1,2</sup>, Sen Yang<sup>1,\*</sup>, Wen Feng<sup>1</sup>, Yan Li<sup>2</sup> and Ye Cheng<sup>2</sup>

<sup>1</sup> School of Materials Science and Engineering, Nanjing University of Science and Technology, Nanjing, 210094, China

<sup>2</sup> School of Material Science and Engineering, Jiangsu University of Science and Technology, Zhenjiang 212330, China

\*E-mail: [guoyuhang@126.com](mailto:guoyuhang@126.com)

Received: 30 March 2016 / Accepted: 3 May 2016 / Published: 4 June 2016

---

The inhibition effect of a Schiff base N'-bis (2-pyridylmethylidene)-1,2-diiminoethane (BPMDE) on AZ31 magnesium alloy was studied in this work. Results showed the BPMDE acts as an effective inhibitor for magnesium in 0.01 M HCl. Potentiodynamic polarization characterization revealed the BPMDE inhibits both anodic and cathodic reactions, indicating the BPMDE acts as a mixed-type corrosion inhibitor behavior. Due to the increasing of adsorption of BPMDE on magnesium alloy surface, the charge transfer resistance consequently increased while the double layer capacitance declined. Moreover, the adsorption of BPMDE on the AZ31 magnesium alloy surface obeys the Langmuir isotherm.

---

**Keywords:** AZ31 magnesium alloy; N'-bis (2-pyridylmethylidene)-1,2-diiminoethane; Corrosion Langmuir isotherm; Inhibitor

### 1. INTRODUCTION

Magnesium and magnesium alloy is one of the lightest metallic alloys have been widely used. The density of magnesium alloy only one quarter and two-thirds of the steel and aluminum, respectively. Despite the low density, the magnesium alloy also exhibits a high mechanical stiffness [1]. Magnesium alloy is a desirable material for aerospace and transportation as well as sporting instrument usage due to its outstanding anti-shock resistance and high strength [2]. However, the application of magnesium alloy was largely restricted by its high corrosion rate compare with than of the steel and aluminum due to its high chemical reactivity. Therefore, the magnesium alloy cannot be applied for various corrosive environment applications. Therefore, developing corrosion protection

technology is essential for magnesium alloy in order to make it capable for wide applications [3, 4]. Among the corrosion protection approaches, addition of inhibitors is one of the most practical approaches, especially when the magnesium alloy expose in an acidic media condition. Corrosion inhibitor is a kind of chemical could largely decrease the corrosion process. Although the additional corrosion inhibitor is the common way for protecting corrosion generates in the metal surface, the performance of the corrosion inhibitor in magnesium alloy has not been widely studied due to the relatively high rate of the corrosion process. A limited number of studies focused on the corrosion inhibition effect of different magnesium alloys using corrosion inhibitor. For example, Dang and co-workers demonstrated the inhibition effect of sodium alginate on magnesium alloy in sodium chloride solution [5]. They found the corrosion process of AZ31 magnesium alloy could be effectively inhibited using sodium alginate. The inhibition efficiency showed an enhancement when the addition of sodium alginate increasing and then declined after further introduction of sodium alginate. The best concentration of adding sodium alginate is 500 ppm. Yang and co-workers investigated the inhibition effect of polyaspartic acid on WE43 magnesium alloy [6]. They found the corrosion process of WE43 magnesium alloy could be effectively inhibited using polyaspartic acid. The best performance of the concentration of the polyaspartic acid has found to be 400 ppm.

Schiff base is a kind of compound contains azomethine group, which received lots of attentions in developing advanced corrosion inhibitor. These compounds have widely investigated as corrosion inhibitors for metals [7-14]. The inhibition performance of the inhibitor not only depended on the structure of the inhibitor but also relate to the nature of the metal and environment. Moreover, the choice of the inhibitor also requires the consideration of the economic aspect. Therefore, the selection of inhibitor candidate is a difficult task.

Acidic environment, such as HCl pickling solution is a common process of most of the metal product. Therefore, reduction of corrosion rate of the metallic materials in HCl pickling solution is important of design a corrosion inhibitor [15, 16].

In this work, a Schiff base *N'*-bis (2-pyridylmethylidene)-1,2-diiminoethane (BPMDE) was synthesized as a corrosion inhibitor for AZ31 magnesium alloy corrosion protection. The corrosion inhibition effect of the BPMDE was studied on the AZ31 magnesium alloy surface in hydrochloric acid solution. Potentiodynamic polarization, electrochemical impedance spectroscopy and electrochemical noise characterizations were carried out for analysis.

## 2. EXPERIMENTS

### 2.1. Materials

Schiff base *N'*-bis (2-pyridylmethylidene)-1,2-diiminoethane (BPMDE) was synthesized according to the reference [17]. Typically, 20 mL 2-pyridinecarbaldehyde (20 mM) ethanol solution was added into 10 mL ethylenediamine (10 mM) ethanol solution under 2 h magnetic stirring. Crude BPMDE was obtained after evaporation of ethanol. The purification process was carried out by recrystallization from petroleum ether. AZ31 magnesium alloy was purchased from local constructional

materials market. Table 1 shows the composition of AZ31 magnesium alloy. For corrosion experimental study, the AZ31 magnesium alloy was polished into  $1\text{ cm} \times 1\text{ cm} \times 1\text{ cm}$  and mounted in polyester that only  $1\text{ cm}^2$  of the surface was in contact with the corrosive solution. Solution of HCl with concentration of 0.05 M was prepared. For immersion corrosion testing, the test method consisted of immersing the specimens in an aquarium filled with HCl solution with and without inhibitor at room temperature. All other chemicals were analytical grade used without further purification.

**Table 1.** Chemical composition of AZ31 magnesium alloy

Elements	Al	Zn	Mn	Si	Cu	Ca	Fe	Ni	Other	Mg
(%)	2.5-3.5	0.7-1.3	0.2	0.05	0.05	0.04	0.005	0.005	0.3	Balance

## 2.2. Electrochemical characterization

All electrochemical characterizations were carried out at a Microautolab3 potentiostat-galvanostat at room temperature under ambient pressure without stirring. Three electrodes system were used for electrochemical impedance spectroscopy (EIS) and polarization measurement, where AZ31 magnesium alloy specimen as working electrode, a platinum wire as the counter electrode and a 3 M Ag/AgCl electrode as reference electrode. The EIS was carried out under potentiostatic condition at corrosion potential with a peak amplitude of 10 mV. The frequency range was set as 1 MHz–10 mHz. The polarization measurement, the scan rate was set as 1 mV/s. For electrochemical noise measurement, two identical AZ31 magnesium alloy specimens and a 3 M Ag/AgCl electrode were used as dual working electrodes and a reference electrode, respectively. Electrochemical current noise was recorded between the two AZ31 magnesium alloy specimens and simultaneously, the potential fluctuations of two short circuited working electrodes were measured with respect to the reference electrode. All other parameters were used same as the reference [18].

## 2.3. Morphology characterization

The morphology of AZ31 magnesium alloy before and after the corrosion process was observed by a scanning electron microscope (SEM, Quanta 200, FEI Coropration, Holland).

## 3. RESULTS AND DISCUSSION

Before electrochemical characterization, the mass loss experiment was conducted by immersing AZ31 magnesium alloy specimens into 0.05 M HCl solution with different concentrations of BPMDE. After 24 h immersion, the corrosion products were removed and the weight of the specimens was recorded. Table 2 shows the average mass loss of AZ31 magnesium alloy specimens after immersion of 0.05 M HCl solution with different concentrations of BPMDE. It can be clearly

seen that the mass loss of AZ31 magnesium alloy decreased along with inhibitor concentration increasing. The corrosion rate was calculated based on the mass loss data according to the following equation:

$$v \text{ (mm/year)} = \frac{8.76 \times 10^4 \times \Delta m}{A \times D \times t}$$

Where A is the surface area of the AZ31 magnesium alloy specimen; D is the density of the AZ31 magnesium alloy; t is the immersion time. The corrosion rate also showed a linear proportion towards mass loss, suggesting the azomethine group and aromatic cycles of the BPMDE could effectively form a preventive layer on the AZ31 magnesium alloy surface. We also calculated the inhibition efficiency and the degrees of surface coverage based on the mass loss data. The degrees of surface coverage and the inhibition efficiency can be deduced using the following questions:

$$\theta = (\Delta m_n - \Delta m_i) / \Delta m_n$$

$$\eta = [(\Delta m_n - \Delta m_i) / \Delta m_n] \times 100\%$$

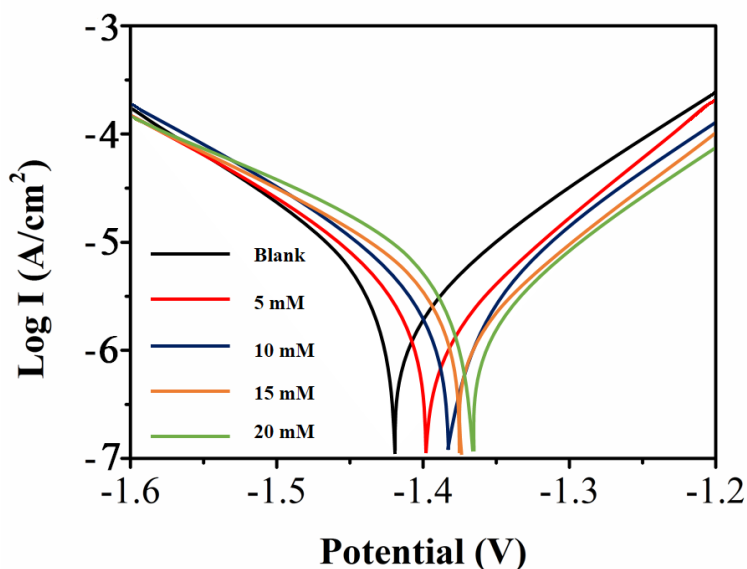
Where the  $\Delta m_n$  is the mass loss without inhibitor while the  $\Delta m_i$  is the mass loss with inhibitor. The maximum inhibition efficiency was recorded when adding 20 mM BPMDE. The reasons of the increasing of the inhibition efficiency with the concentration of BPMDE increasing can be described as follow: the addition of high concentration of BPMDE increased the surface coverage as well as inhibitor efficiency due to the adsorption. The adsorption could be achieved through the electrostatic interaction between protonated nitrogen atoms and the  $\text{MgCl}_2^-$  formed on the AZ31 magnesium alloy surface under HCl condition. The chemisorption of the BPMDE also contributes the inhibition performance as well through interaction of  $\pi$  orbitals between BPMDE and metal surface. Based on the mass loss experiment, the BPMDE showed an excellent performance as an inhibitor.

**Table 2.** Weight loss data for AZ31 magnesium alloy using different concentrations of BPMDE.

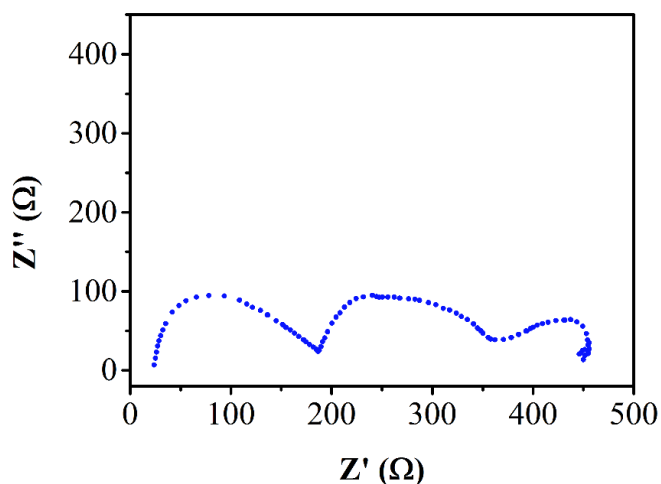
Concentration of BPMDE (mM)	Mass loss (g)	Corrosion rate (mm/year)	Inhibition efficiency (%)	Surface coverage
No BPMDE	7.22	19.88	—	
5	4.81	12.45	25.41	0.2541
10	4.21	10.41	37.89	0.3789
15	3.56	9.67	50.19	0.5109
20	2.77	7.30	62.23	0.6223

Figure 1 shows the potentiodynamic polarization profiles of AZ31 magnesium alloy specimens in 0.05 M HCl solution with different concentrations of BPMDE. It can be seen that the both anodic and cathodic responses showed a clear decline when the BPMDE added into system, suggesting the BPMDE reduced the anodic dissolution process and retards the hydrogen evolution reaction. The corrosion potential ( $E_{\text{corr}}$ ) showed a continuous shifted to more positive value when the concentration of BPMDE increasing. As the shift of the  $E_{\text{corr}}$  was less than 85 mV, the BPMDE can be assigned as a mixed type inhibitor [19, 20]. Other electrochemical corrosion parameters such as cathodic and anodic

Tafel slopes, corrosion potential and corrosion current density were also obtained from polarization curves (Table 4). It can be seen that no significant cathodic and anodic Tafel slopes changes were observed after addition of the BPMDE, suggesting the mechanism of magnesium dissolution and hydrogen evolution has not been changed. The inhibition efficiency had a good agreement with the value recorded in the weight loss measurement. Therefore, the inhibition performance of the BPMDE is mainly due to the surface adsorption, which blocking the active corrosion sites [7]. The inhibition efficiencies were then calculated based on measured polarization resistance of each profile. The inhibition efficiency of 5, 10, 15 and 20 mM BPMDE addition were calculated to be 26.41, 40.12, 52.56 and 67.89 %, respectively, which had a good agreement with the values deduced from weight loss measurement.



**Figure 1.** Potentiodynamic polarization profiles of AZ31 magnesium alloy in 0.05 M HCl solution with different concentrations of BPMDE addition.



**Figure 2.** Nyquist plots of AZ31 magnesium alloy in the 0.05 M HCl solution at corrosion potential.

**Table 4.** Polarization parameters for AZ31 Mg alloy in 0.05 M HCl with different concentrations of BPMDE addition

BPMDE concentration (mM)	Anodic slope (mV/dec)	Cathodic slope (mV/dec)	Corrosion potential (V)	corrosion density (A/cm <sup>2</sup> )	Inhibitor Efficiency (%)
0	137	142	-1.423	54.7	none
5	135	147	-1.399	42.8	28.54
10	148	143	-1.382	31.2	39.92
15	163	159	-1.371	19.6	51.21
20	153	154	-1.360	7.3	64.09

For further analysis, electrochemical impedance spectroscopy was applied for obtaining additional information of the inhibition process. Figure 2 shows the Nyquist plots of AZ31 magnesium alloy specimens in 0.05 M HCl solution without addition of BPMDE. From the Nyquist plots, three well-defined capacitive loops and a scattered inductive loop could be observed. The scattered inductive loop at low frequency range can be assigned to the partially protective surface film. The third capacitive loop can be assigned to the Mg<sup>+</sup> ion concentration within the film free area [21], which only occurs in the formation of the partially protective surface film. The second capacitive loop can be assigned to the charge transfer resistance and the double layer capacitance of AZ31 magnesium alloy surface [22, 23]. The first capacitive loop can be assigned to the non-faradaic processes adsorption of hydrogen ions [24].

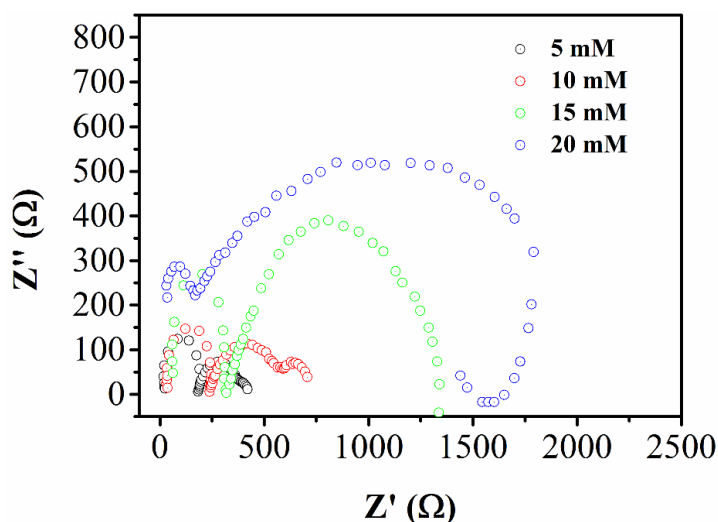


**Figure 3.** Nyquist plots of AZ31 magnesium alloy in the 0.05 M HCl solution with addition of 5, 10, 15 and 20 mM BPMDE.

Figure 3 shows the Nyquist plots of AZ31 magnesium alloy specimens in 0.05 M HCl solution with different concentration of BPMDE. It can be observed that the diameter of the second capacitive loop in the Nyquist plots showed clearly increasing when the BPMDE concentration increasing,

suggesting high inhibition ability of the BPMDE on AZ31 magnesium alloy corrosion in acidic media. For the high concentration of BPMDE addition, the corresponding Nyquist plots showed clear enhancement of the charge transfer resistance by a well-defined capacitive loop at highest frequencies with two scarcely defined capacitive loops at high and medium frequencies, due to the high content of BPMDE adsorbed on the AZ31 magnesium alloy surface.

We further analysed the electrochemical current noise and electrochemical potential noise of the AZ31 magnesium alloy after 1 h of immersion in the 0.05 M/L HCl solution with different concentrations of BPMDE. Figure 4 shows the a typical electrochemical noise records of AZ31 magnesium alloy in 20 mM of BPMDE. We analyzed the electrochemical current noise and electrochemical potential noise data of no BPMDE sample, 5 mM and 20 mM BPMDE samples, respectively. Noise resistance was calculated as the ratio of the standard deviation of potential noise,  $\sigma_V$  to that of current noise,  $\sigma_I$ . The noise resistances of control group, 5 mM BPMDE sample and 20 mM BPMDE sample were calculated to be 425  $\Omega$ , 788  $\Omega$  and 3650  $\Omega$ , respectively. A clear enhancement of noise resistance was observed after addition of BPMDE, suggesting the more BPMDE adsorption on the AZ31 magnesium alloy surface.

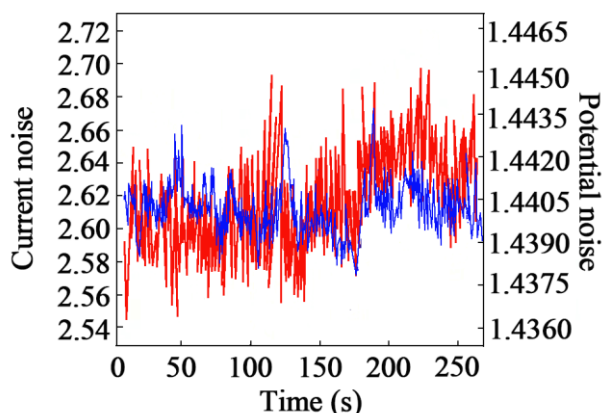


**Figure 4.** Typical electrochemical noise records of AZ31 magnesium alloy in 20 mM of BPMDE.

As the BPMDE inhibition was achieved through adsorption. We further analysed the adsorption isotherm of the adsorption of BPMDE on AZ31 magnesium alloy surface. The surface coverage data was used for fitting different adsorption isotherm including Freundlich, Langmuir, Temkin isotherms. Study showed the Freundlich isotherm had best fitting for existing data. Figure 5 shows the plot of logarithm of surface coverage versus logarithm of concentration. The Freundlich isotherm equation can be expressed as:  $y(\text{Log}_{\text{surface coverage}}) = 1.005x(\text{Log}_{\text{concentration}}) + 2.733$ . The adsorption free energy can be then calculated according to following equation [18]:

$$\Delta G_{ads} = -RT \log(K_{ads})$$

The adsorption free energy was calculated to be -21.44 kJ/mol, suggesting the adsorption mainly caused by the electrostatic interaction between the AZ31 magnesium alloy surface and BPMDE [25]. Therefore, under an acidic condition,  $\text{Cl}^-$  was adsorbed onto the positively charged AZ31 magnesium alloy surface via columbic attraction. Then, the protonated BPMDE can be adsorbed on the AZ31 magnesium alloy surface through electrostatic interaction [26].

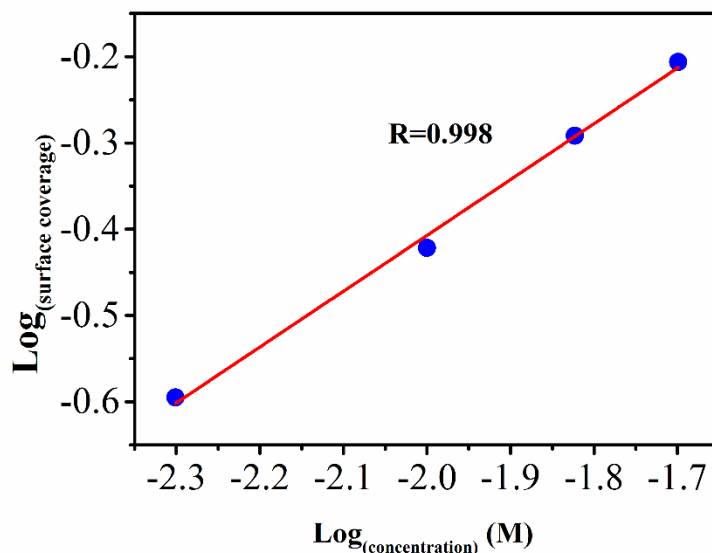


**Figure 5.** Freundlich adsorption isotherm plot.

SEM was used for analysing AZ31 magnesium alloy surface morphology after addition of the inhibitor. Figure 6 A and B shows the SEM image of the AZ31 magnesium alloy after 2 h of immersion in 0.05 M HCl in the absence and presence of 0.02 M BPMDE, respectively. As shown in the Figure 6A, the metallic surface had a strong damage when no inhibitor protection. Clear metal dissolution can be observed. On the other hand, the damage of the metal surface showed a diminishment when the presence of 0.02M BPMDE, further confirming the formation of a protective film by adsorption of BPMDE.

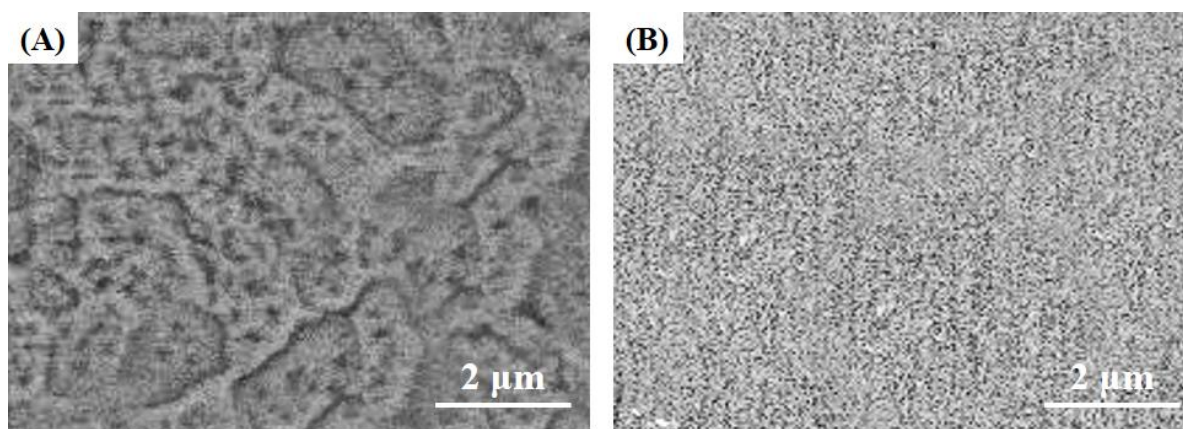


**Figure 6.** SEM image of AZ31 magnesium alloy surface after immersion of 0.05 M HCl for 2 h (A) in the absence of BPMDE and (B) in the presence of 0.02 M BPMDE.

#### 4. CONCLUSION

In this work, we successfully synthesized Schiff base BPMDE as a corrosion inhibitor for AZ31 magnesium alloy surface protection. Study showed the BPMDE exhibited an effective



performance towards AZ31 magnesium alloy surface corrosion. The influence of the BPMDE concentration was investigated in detail. Weight loss measurement and potentiodynamic polarization characterization showed the increasing of concentration can enhance the inhibition performance. EIS and electrochemical noise analysis further confirmed the statement. The inhibition performance of the BPMDE can be ascribed to the strong adsorption property. SEM surface morphology analysis also displayed the inhibition role of the BPMDE.

## References

1. J. Hu, D. Huang, G.-L. Song and X. Guo, *Corrosion Science*, 53 (2011) 4093
2. J. Sudagar, J.-S. Lian, X.-m. Chen, L. Peng and Y.-q. Liang, *Transactions of Nonferrous Metals Society of China*, 21 (2011) 921
3. H. Zhao, Z. Huang and J. Cui, *Surface and Coatings Technology*, 202 (2007) 133
4. D. Seifzadeh and Z. Rajabalizadeh, *Surface and Coatings Technology*, 218 (2013) 119
5. N. Dang, Y.H. Wei, L.F. Hou, Y.G. Li and C.L. Guo, *Materials and Corrosion*, 66 (2015) 1354
6. L. Yang, Y. Li, B. Qian and B. Hou, *Journal of Magnesium and Alloys*, 3 (2015) 47
7. H. Ashassi-Sorkhabi, B. Shaabani and D. Seifzadeh, *Appl. Surf. Sci.*, 239 (2005) 154
8. H. Ashassi-Sorkhabi, B. Shaabani and D. Seifzadeh, *Electrochimica Acta*, 50 (2005) 3446
9. R. Solmaz, E. Altunbaş and G. Kardaş, *Mater. Chem. Phys.*, 125 (2011) 796
10. H. Ashassi-Sorkhabi, B. Shabani, B. Aligholipour and D. Seifzadeh, *Appl. Surf. Sci.*, 252 (2006) 4039
11. M. Behpour, S. Ghoreishi, M. Salavati-Niasari and B. Ebrahimi, *Mater. Chem. Phys.*, 107 (2008) 153
12. L. Fu, Y. Zheng, A. Wang, W. Cai, B. Deng and Z. Zhang, *Arab J Sci Eng*, 41 (2016) 135
13. Y. Zheng, L. Fu, F. Han, A. Wang, W. Cai, J. Yu, J. Yang and F. Peng, *Green. Chem. Lett. Rew.*, 8 (2015) 59
14. L. He, L. Fu and Y. Tang, *Catalysis Science & Technology*, 5 (2015) 1115
15. S. Issaadi, T. Douadi, A. Zouaoui, S. Chafaa, M. Khan and G. Bouet, *Corrosion Science*, 53 (2011) 1484
16. S. Xu, L. Fu, T.S.H. Pham, A. Yu, F. Han and L. Chen, *Ceram. Int.*, 41 (2015) 4007
17. H. Shekaari, A. Bezaatpour and M. Khoshalhan, *Thermochimica Acta*, 527 (2012) 67
18. H. Ashassi-Sorkhabi, D. Seifzadeh and M. Hosseini, *Corrosion Science*, 50 (2008) 3363
19. W.-h. Li, Q. He, S.-t. Zhang, C.-l. Pei and B.-r. Hou, *Journal of Applied Electrochemistry*, 38 (2008) 289
20. V.V. Torres, R.S. Amado, C.F. de Sá, T.L. Fernandez, C.A. da Silva Riehl, A.G. Torres and E. D'Elia, *Corrosion Science*, 53 (2011) 2385
21. G. Song, A. Atrens, D. St John, X. Wu and J. Nairn, *Corrosion Science*, 39 (1997) 1981
22. C.-N. Cao, *Electrochimica Acta*, 35 (1990) 831
23. C.-N. Cao, *Electrochimica acta*, 35 (1990) 837
24. M.C. Turhan, R. Lynch, M.S. Killian and S. Virtanen, *Electrochimica Acta*, 55 (2009) 250
25. S. Şafak, B. Duran, A. Yurt and G. Türkoğlu, *Corrosion Science*, 54 (2012) 251
26. M. Lagrenee, B. Mernari, M. Bouanis, M. Traisnel and F. Bentiss, *Corrosion Science*, 44 (2002) 573